

Observation of the $i = \frac{1}{2}$ fractional quantum Hall plateau in AlGaAs/GaAs/AlGaAs selectively doped double heterostructures

P E Lindelof, H Bruust†, R Taboryski and C B Sørensen

Physics Laboratory, H C Orsted Institute, Universitetsparken 5,
2100 Copenhagen O, Denmark

Received 18 January 1989, in final form 28 April 1989, accepted for publication
1 June 1989

Abstract. An inverted and a normal GaAs/AlGaAs interface grown back to back in a selectively doped double heterostructure (SDDH) has been studied in magnetic fields up to 12 T and at temperatures down to 0.3 K. The longitudinal resistance goes to zero at the minima of the Shubnikov–de Haas oscillations. The Hall resistivity is found to exhibit the quantum Hall effect. By etching the surface of the double heterostructure wafer we create an imbalance in the density of electrons in the two parallel two-dimensional electronic sheets. Although in this way we create only a modest change in the electron densities, we observe a significant change in the Shubnikov–de Haas oscillations, which can be interpreted as a beat between the oscillations of two electron layers with different densities. At the same time we observe a significant variation of the width of the quantum Hall steps. The most astonishing feature of our results is a clear quantum Hall plateau at $\frac{1}{2}$ filling in each of the two parallel layers observed at temperatures below 1 K and at a magnetic field above 10 T. Weak localisation was also studied and such experiments are consistent with two parallel and independent two-dimensional electronic layers.

1. Introduction

Whereas experimentally the quantum Hall effect at integer and fractional plateau values appear to be closely related physical phenomena, the theoretical pictures of the two phenomena are very different indeed (for a review see Aoki (1987)). The integer quantum Hall effect is explained in the independent semiclassical electron model, whereas the fractional quantum Hall effect is described by an incompressible charged quantum fluid. One of the characteristic features of the integer quantum Hall effect is its basic nature, which appeals to many apparently different theoretical pictures. Although many-body effects seem crucial for the description of the fractional quantum Hall effect, in this case the theoretical picture is also misty. In view of this situation new types of experiments are urgently needed. In this publication we report low-temperature experiments on the AlGaAs/GaAs/AlGaAs double heterostructures schematically represented in figure 1. Two two-dimensional (2D) electron layers are in close proximity and with no disturbing donors between the layers or in the immediate vicinity of the layers.

The quantum Hall effect has been studied previously in

multilayer or superlattice heterostructures. In most cases (Nicholas *et al* 1982, Eisenstein *et al* 1985) the many 2D electron layers are too far apart to interact, and the quantum Hall resistance is simply scaled down by the number of independent parallel layers. In one previous publication (Störmer *et al* 1986) 30 layers were prepared in close proximity. In this case well developed quantum Hall plateaus were observed, but only corresponding to 24 parallel layers. This experimental observation is explained by the unavoidable inhomogeneities in the layers, yet it is difficult to understand why the quantum Hall effect is then so well developed. Studies of the optical properties of a discrete number of 2D electron layers have also been carried out (Pinczuk *et al* 1986, Fasol *et al* 1986). In these cases discrete plasmons are clearly observed showing interlayer coupling. In all these cases donor atoms were squeezed in between the individual layers in order to create the electron sheets at the GaAs–AlGaAs boundaries.

The GaAs/AlGaAs heterostructure used in our experiment had two GaAs–AlGaAs boundaries creating two electron layers in the same 40 nm thick GaAs channel, as illustrated in figure 1. Outside the channel there is a 15 nm intrinsic spacer layer on either side. The two 2D electron layers are therefore far removed from any donors and constitute an experimental realisation of two electronic sheets placed in a dielectric background mater-

†Permanent address: Danish Institute of Fundamental Metrology,
Bldg 322, Lundtoftevej 100, 2800 Lyngby, Denmark.

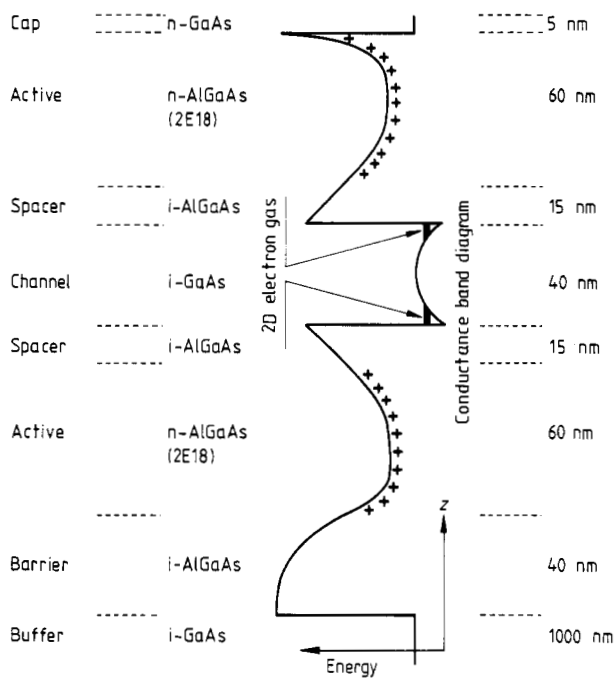


Figure 1. A schematic view of the layer sequence of our GaAlAs/GaAs/GaAlAs selectively doped double heterostructure (SDDH). At the left is seen the names of the different layers and the composition (Si-doping concentration: $2 \times 10^{18} \text{ cm}^{-3}$ and Al mole fraction: 0.30). To the right we show the layer thicknesses. In the middle we show schematically the variation of the conduction band edge through the different layers. The depleted donor atoms are indicated by crosses. The 2D electron layers are indicated in the GaAs quantum well channel at the interfaces. The structure is intended to be symmetric around the GaAs quantum well.

ial. Such a physical system was in fact studied theoretically many years ago by Visscher and Falicov (1971). In recent years a number of theoretical papers have been concerned with the physical properties of coupled layers of 2D electrons (Chakraborty and Pietiläinen 1987, Que and Kirzenow 1987, Vinter and Tardella 1987, Hawrylak *et al* 1988, Santoro and Giuliani 1988, Yang *et al* 1988). The selectively doped double heterostructure (SDDH) was invented due to its interesting potentialities for high electron mobility transistors (HEMTs) (Inoue *et al* 1984) Until recently, only little attention has been paid to its basic physical properties (Harris *et al* 1988). We therefore considered it worthwhile to study this structure.

2. The selectively doped double heterostructure

The layer sequence of our selectively doped double heterostructure (SDDH) is shown in figure 1. The heterostructure was grown by the molecular beam epitaxy (MBE) technique on a modular Varian Gen II apparatus. The structure is built up symmetrically around the GaAs channel where the two sheets of 2D electron layers are situated on either side. A $1 \mu\text{m}$ GaAs buffer layer was first grown on the GaAs substrate. On top of this a 40 nm

$\text{Al}_{0.30}\text{Ga}_{0.70}\text{As}$ intrinsic layer was grown to avoid a charged layer at this interface. The substrate temperature was 610°C during this part of the epitaxial growth. The temperature was then increased to 680°C , and the rest of the layers were grown. The next five epitaxial layers were grown in such a way that a 40 nm GaAs middle channel layer was meant to hold the electrons from two active $\text{Al}_{0.30}\text{Ga}_{0.70}\text{As}$ layers which both had a thickness of 60 nm and a Si concentration of $2 \times 10^{18} \text{ cm}^{-3}$. Between the channel layer and the two active layers two 15 nm thick intrinsic $\text{Al}_{0.30}\text{Ga}_{0.70}\text{As}$ spacer layers were grown in order to separate the donors from the electronic layers (modulation doping). Finally a 5 nm thick GaAs cap layer was grown on the top of the heterostructure to facilitate the fabrication of ohmic contacts. In figure 1 we have also sketched the position of the conduction band minimum as a function of position through the layers. The electrons are caught in two triangular wells on either side of the GaAs channel and form two 2D electronic layers. The electronic wavefunctions have an extension perpendicular to the planes of about 5 nm as sketched in figure 1. The position of the 2D electronic layers and the electronic density within them are in principle calculable from Poisson's and Schrödinger's equations (Inoue *et al* 1984, Miyatsuji *et al* 1985). In the double heterostructure, any asymmetry will easily tilt the electronic distribution in the channel layer from one side to the other (Miyatsuji *et al* 1985, Vinter and Tardella 1987).

The heterostructure wafer was cut into $6 \times 12 \text{ mm}^2$ chips, and by use of standard photolithography and wet-etch techniques, a mesa-etched $0.2 \times 4 \text{ mm}^2$ Hall bar was made in the surface of each chip. The contact pads consisted of evaporated and annealed AuGeNi films (Nørregaard *et al* 1987). The contact pads extended outside the Hall mesa to avoid losing contact to the 2D electrons in high magnetic fields by an unintentional Corbino geometry. The chip was placed on a chip carrier and the contact pads were Au-bonded. The chip carrier was then placed in an Oxford Instruments top-loading ^3He cryostat with a 12 T magnet installed. At room temperature there was a significantly thermally activated charge transport in the bulk of the heterostructure, whereas at low temperature we found only contributions to the conductance from the 2D electronic layers. From the Hall effect and the Shunikov-de Haas oscillations we found the total electron concentration in the two layers to be $3.2 \times 10^{15} \text{ m}^{-2}$ and the average mobility to be $1.3 \text{ m}^2 \text{ V}^{-1} \text{ s}^{-1}$. It is well known that inverted GaAlAs/GaAs heterostructures have much lower electron mobilities at low temperatures than normal heterostructures. The substrate temperature during the growth plays an important role for the perfection of the inverted interface, but it also leads to a smearing of the Si impurity profile, since the Si donor atoms in the GaAlAs migrates at elevated temperatures (Inoue *et al* 1985). Large differences between the mobility of the electrons on the two sides of the GaAs quantum well have been reported in the literature (Harris *et al* 1988) and can be ascribed to the large defect density at the inverted interface. We have grown our wafer at a relatively high temperature and

therefore expect a relatively lower mobility at both interfaces. The low mobility in our sample is, however, primarily a consequence of the low carrier concentration as we shall demonstrate below.

In order to change the condition of the SDDH we etched the surface with a very dilute mixture of 4⁰/₀₀ NH₄(25%) and 1.6⁰/₀₀ H₂O₂(30%) in water. The etching rate was not very well controlled and became worse with more dilute solutions. An etching time of about 5–10 s made the heterostructure completely insulating. We therefore etched a number of chips for a few seconds and compared the the electrical properties of these different samples, which were all taken from the same wafer, however. Since the thickness of the GaAs channel layer is only 40 nm, contacting the two 2D layers individually was not feasibly. In figure 2 we have plotted the resistance per square of the two layers as a function of the charge-carrier density determined from the Hall effect and the Shubnikov–de Haas effect. Sample A represents the unperturbed samples, whereas the other samples are the result of a slight etch in the surface. The resistance increases roughly inversely proportional to the carrier density squared, indicating a relaxation rate which increases inversely proportional to the carrier density. This behaviour is a result of a reduced screening of the charged impurities as the carrier density is reduced.

3. The Shubnikov–de Haas oscillations and the quantum Hall effect

In figures 3 and 4 we plot the resistance per square and the Hall resistance as a function of magnetic field for samples A, B and C (compare figure 2). Sample A corresponds to the intrinsic wafer described in the previous section. As seen, this unetched SDDH exhibits a clear B^{-1} Shubnikov–de Haas oscillation corresponding to only one type of charge carrier with a total concentration of $3.2 \times 10^{15} \text{ m}^{-2}$, i.e. $1.6 \times 10^{15} \text{ m}^{-2}$ per 2D layer. Samples B and C were etched as described above. All the differently etched samples were consistent in that a meaningful family of curves such as shown in figure 3 was found for all samples. The chemical wet etch first removed the GaAs cap layer and then the active Al_{0.30}Ga_{0.70}As top layer. The etching therefore introduced an imbalance between the 2D layers. This is clearly seen in the recordings shown in figure 3, where the regular B^{-1} oscillation of sample A indicating two almost identical layers is replaced in samples B and C by an aperiodic oscillation which we interpret as the sum of two Shubnikov–de Haas oscillations. In order to demonstrate how the magnetoresistance curves of samples B and C in figure 3 are formed, we have calculated two similar curves in figures 5(b) and (c) in the following way: the experimental curve in 5(a) (the same as for sample A in figure 3) is resolved into two parallel and identical resistors. These two parallel magnetoresistances are then changed differently by scaling the magnetic field axes, in order to have the two Shubnikov–de Haas oscillations corresponding to the two differently reduced charge-

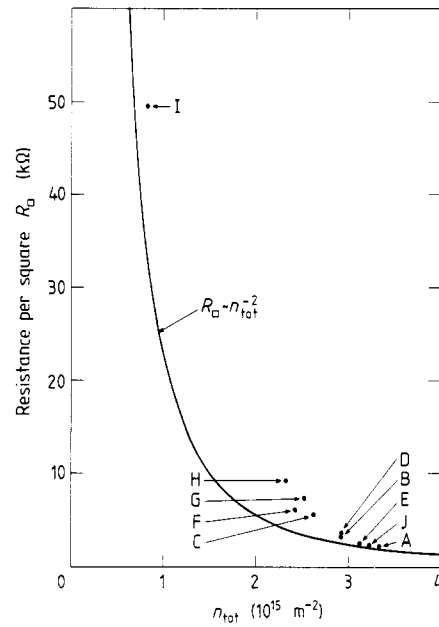


Figure 2. Resistance per square for a selectively doped double heterostructure (SDDH) for different surface etching plotted as a function of the total electron density, n_{tot} . The total electron density is determined by the Hall or Shubnikov–de Haas effect. All the different samples obtained by etching lie on one curve (shown), which can be roughly described by a n_{tot}^{-2} law. The samples A, B, C, D, F and G will be used for subsequent figures. $T = 0.35 \text{ K}$, $B = 0$.

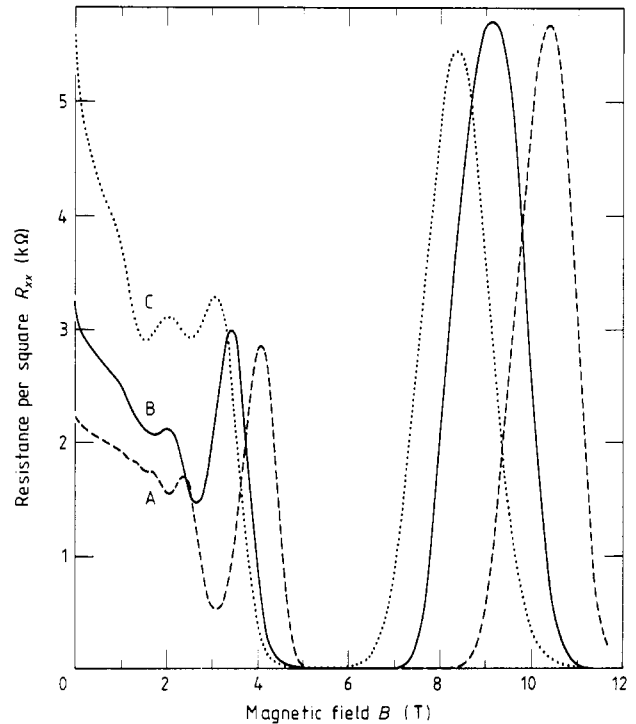


Figure 3. Resistance per square, R_{xx} , for three differently etched SDDH samples (A, B, C) recorded as a function of magnetic field. $T = 0.32 \text{ K}$. Whereas sample A (not etched) exhibits a regular Shubnikov–de Haas oscillation that is periodic in B^{-1} , samples B and C have a beat in the oscillation, which we interpret as evidence for the existence of two sets of charge carriers. Sample A is estimated to have a charge carrier density of $3.2 \times 10^{15} \text{ m}^{-2}$.

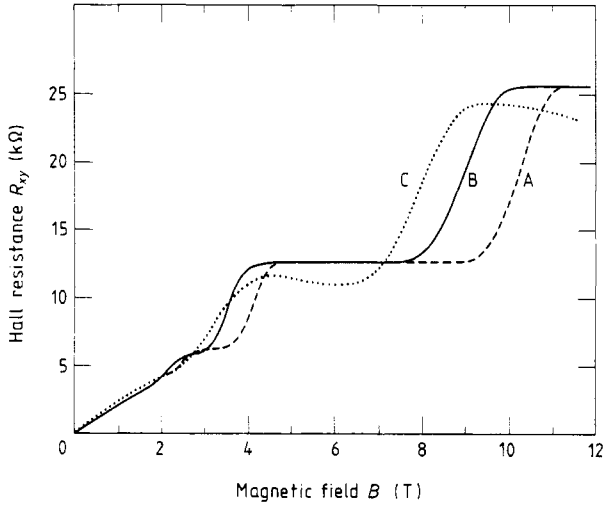


Figure 4. Hall resistance of three differently etched SDDH samples (A, B, C) recorded as a function of magnetic field. $T = 0.32$ K. Sample A is not etched and has a very wide $R_{xy} = 12.9$ k Ω quantum Hall plateau which stretches from 4.5 to 9T. Since there are two 2D electron layers the $R_{xy} = 25.8$ k Ω quantum Hall plateau corresponds to a fractional plateau, $R_{xy} = h/(ie^2)$, with $i = \frac{1}{2}$, in each of the two layers. Sample C, which has a 40% asymmetry between the two 2D electron layers exhibits a greatly degraded quantum Hall plateau.

carrier densities. Indeed the parallel combination of the two magnetoresistance curves resembles the experimental curves in figure 3 for samples B and C. It should be noticed that we have kept the resistance at $B = 0$ constant under this transformation, contrary to the experiment where the resistance rises quickly with decreasing charge carrier density (see figure 2). The fact that we observe both oscillations for the two different carrier densities indicates that the mobility of the electrons in the

two 2D layers are very similar. In this respect our results differ from those obtained by Harris *et al* (1988), where the top 2D layer has a mobility 10 times higher than the bottom (inverted) layer. As mentioned above, we believe that this is due to our high substrate temperature during growth and our low electron concentration. Sample C is estimated from Shubnikov-de Haas oscillations to have the following electron concentration in the two layers: $1.4 \times 10^{15} \text{ m}^{-2}$ and $1.0 \times 10^{15} \text{ m}^{-2}$ respectively. Sample B is intermediate. These values agree with Hall effect measurements. For sample A a magnetic field in excess of 5 T brings the Shubnikov-de Haas oscillations into a quantum Hall regime, where the resistance per square is less than 1% of the zero field value for a magnetic field range of more than 3.5 T. Figure 4 shows measurements on samples A, B and C of the Hall resistivity. The Hall plateau value at $R_{xy} = 12.9$ k Ω means that for sample A each of the two electronic layers is at a $R_{xy} = h/e^2 = 25.8$ k Ω step, i.e. completely spin-polarised. If it were only for the measurement on the precisely balanced SDDH system with two identical electronic layers, we would not be able to distinguish whether we were considering one or two 2D layers. However, our etching experiment reveals the presence of two electronic layers, as was also intended in the growth of the sample. This means that the quantum Hall plateau at $R_{xy} = 25.8$ k Ω , which we observe at even high magnetic fields (above 9 T) corresponds to an $i = \frac{1}{2}$ plateau for each of the two electronic layers. It is noteworthy that the $i = \frac{1}{2}$ and $i = 1$ steps quickly deteriorate as the balance of the carrier densities in the two 2D layers is changed by the etching. This can be taken as a sign of a loss of correlation between the two layers. The fractional $i = \frac{1}{2}$ plateau has been predicted in a calculation by Chakraborty and Pietiläinen (1987). In figures 6 and 7 we show the variation of the resistance per square and the Hall resistance versus magnetic field for another

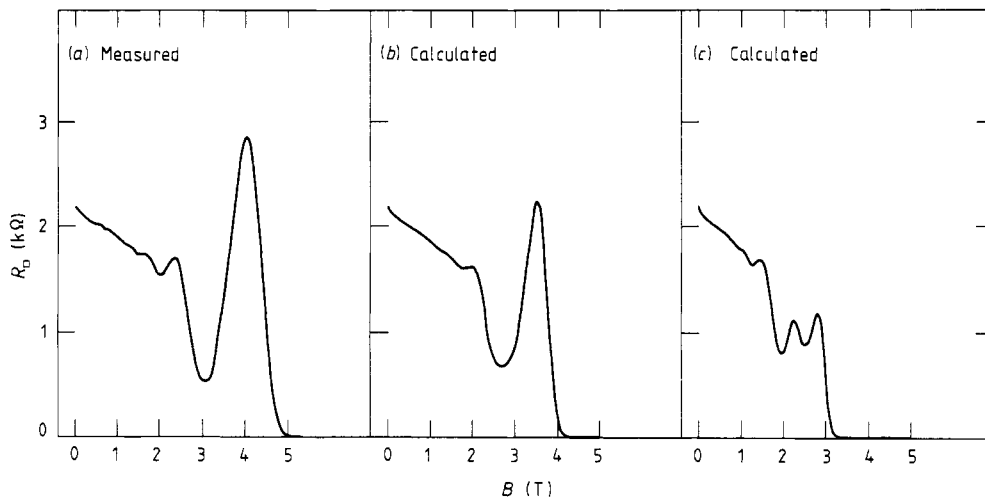


Figure 5. Resistance per square, R_{xx} , as a function of magnetic field. (a) Sample A (same as A in figure 3). The electron densities in each of the two 2D electron layers are $n_1 = n_2 = 1.6 \times 10^{15} \text{ m}^{-2}$. (b) and (c) R_{xx} calculated on the basis of two parallel layers as in (a), but here with two different electron concentrations, i.e. as a sum of two conductance channels identical to the experimental curve in (a) but scaled along the B axis. The figures (b) and (c) should be compared to samples B and C in figure 3. In (b) $n_1 = 1.52 \times 10^{15} \text{ m}^{-2}$, $n_2 = 1.33 \times 10^{15} \text{ m}^{-2}$. In (c) $n_1 = 1.33 \times 10^{15} \text{ m}^{-2}$, $n_2 = 1.03 \times 10^{15} \text{ m}^{-2}$.

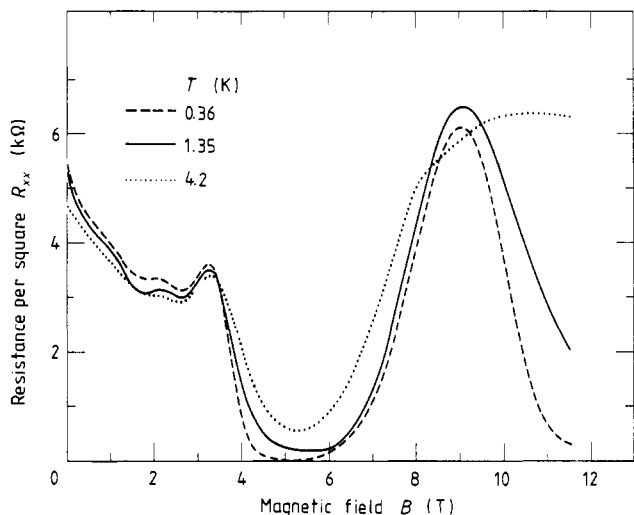


Figure 6. Resistance per square of sample F, which is one of the etched SDDH samples, recorded as a function of magnetic field for three different temperatures.

etched sample taken at three temperatures. As expected, the plateaus deteriorate with increasing temperature. It is interesting however, that the $i = \frac{1}{2}$ step deteriorates considerably faster than the $i = 1$ step. In order to quantify this we have measured the square resistance as a function of temperature for both the $i = \frac{1}{2}$ and $i = 1$ step. The logarithm of the square resistance is plotted in figure 8 as a function of inverse temperature. We would like to extract an activation energy from these measurements, but this is difficult. Measurements such as those shown in figure 8 are often interpreted as activated behaviour at high temperatures, from which a mobility gap is extracted, and a hopping behaviour at low temperatures. If we take the same attitude we can make a rough fit to

exponential behaviour, $R_{\square} \sim \exp(-\Delta/2k_B T)$. This is shown as the full line in figure 8, on both sides of the square resistance 2 kΩ. In this way we find the activation energies $\Delta(i = \frac{1}{2}) \simeq 0.4$ meV ($B = 12$ T) and $\Delta(1) \simeq 2.0$ meV ($B = 5.5$ T). The Landau level splitting at 5.5 T is for comparison $\hbar\omega_c = \hbar e B/m^* \simeq 8$ meV. It should be noted here that we have not reached the middle of the $i = \frac{1}{2}$ fractional plateau at our highest magnetic field, $B = 12$ T, and we therefore expect a slightly higher activation energy in this case. Note also that the $i = \frac{1}{2}$ plateau magnetic field is considerably higher than twice the value obtained at the $i = 1$ plateau. We do not know why this happens. Chakraborty and Pietiläinen (1987) find a splitting of energy at the $i = \frac{1}{2}$ fractional occupation of $\Delta(\frac{1}{2}) = 0.209 e^2/(4\pi\epsilon_0\epsilon_r l_0) \simeq 3$ meV, for a distance between the two layers of $C = 2l_0$, where l_0 is the magnetic length $l_0 = (\hbar e/B)^{1/2} \simeq 7$ nm at $B = 12$ T. It is not clear, however, how wide a mobility gap one should then expect for our sample.

4. Weak localisation results

At low temperatures and in low magnetic fields the negative weak localisation magnetoresistance can be studied. The weak localisation magnetoresistance is normally well described by the theory of Hikami *et al* (1980), in particular in 2D electron layers with low mobilities and high square resistances such as those studied in this work. The quantum correction is, however, particularly interesting for the type of samples studied here, since there is a quantum correction attached to each of the two 2D electron layers. If there is only insignificant tunnelling between the two layers, we expect the quantum correction to double relative to the

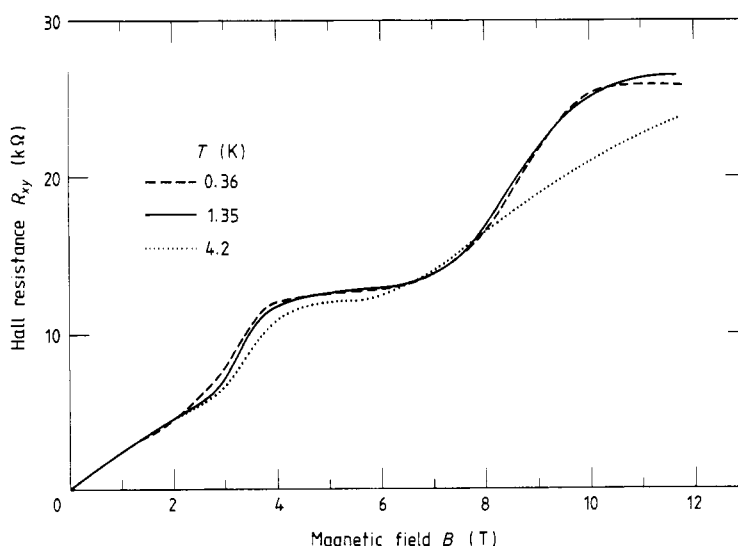


Figure 7. Hall resistance of sample F, which is one of the etched SDDH samples, recorded as a function of magnetic field for three different temperatures. Notice that the quantum Hall plateau at $R_{xy} = 25.8$ kΩ has disappeared at $T = 4.2$ K. The low field slope, i.e. the classical Hall effect, yields the charge carrier density in agreement with the Shubnikov-de Haas effect. However, see figure 9 for a deviation at very low magnetic fields.

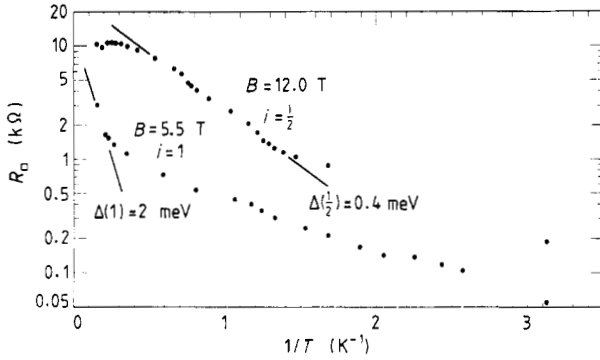


Figure 8. Minimal resistances per square for SDDH sample G at the quantum Hall plateau values $R_{xy} = 12.9 \text{ k}\Omega$ ($i = 1$) and $R_{xy} = 25.8 \text{ k}\Omega$ ($i = \frac{1}{2}$) plotted versus the inverse temperature in a semilogarithmic plot. The minima occur at the magnetic fields $B = 5.5 \text{ T}$ and $B \geq 12 \text{ T}$. The inequality sign indicates that we have not yet reached the resistance minimum at our highest magnetic field for the $i = \frac{1}{2}$ plateau. It is observed that the magnetic field at the $i = \frac{1}{2}$ plateau exceeds twice the field at the $i = 1$ plateau for all samples. We have attempted to deduce activation energies from the indicated straight lines in the resistance region of $2 \text{ k}\Omega$.

expectation based on one combined 2D layer or a situation with a strong coupling between the two layers. In the formula by Hikami *et al* (1980) for the weak localisation conductance correction as a function of temperature T and magnetic field B

$$\Delta\sigma(T, B) = [\alpha e^2/(\pi h)] [\psi(\frac{1}{2} + B_\phi/B) - \psi(\frac{1}{2} + B_0/B)] \quad (1)$$

we have therefore introduced a parameter α , which we have used as a fitting parameter in addition to the characteristic magnetic field $B_\phi = \hbar/(4eD\tau_\phi)$. τ_ϕ is the so-called phase relaxation time. D is the diffusion constant for the 2D electron gas known from the total carrier density n_{tot} and the resistance per square R_\square . Ψ is the digamma function. $B_0 = \hbar/(4eD\tau_0)$, where τ_0 is the transport relaxation time, which is also known from n_{tot} and R_\square . $\alpha = 2$ signals two independent and parallel 2D electronic layers; $\alpha = 1$ only one.

In figure 9 we show recordings of negative magnetoresistance and non-linear Hall resistivity as a function of magnetic field for one of our samples (D) at our lowest temperature. The wiggles in the magnetoresistance are a result of analogue-to-digital conversion in our apparatus. Both experimental traces are a direct consequence of equation (1). By inverting the conductivity tensor to a resistivity tensor and expanding to lowest order in the quantum correction $R_\square \Delta\sigma(T, B)$ and using the simple free-electron model, we obtain the following resistivity components:

$$R_{xx} = R_\square(1 + R_\square \Delta\sigma(T, B)) \quad (2a)$$

$$R_{xy} = R_{xy}(0)(1 + 2R_\square \Delta\sigma(T, B)). \quad (2b)$$

Whereas normally the quantum correction to the resistance is very tiny, because $(\pi h)/e^2 = 81 \text{ k}\Omega$, it is quite sizable in this case since R_\square is larger than about $2 \text{ k}\Omega$ as seen in figure 2. However, for sample D the expansion in equation (2) is still valid. The fact that the quantum

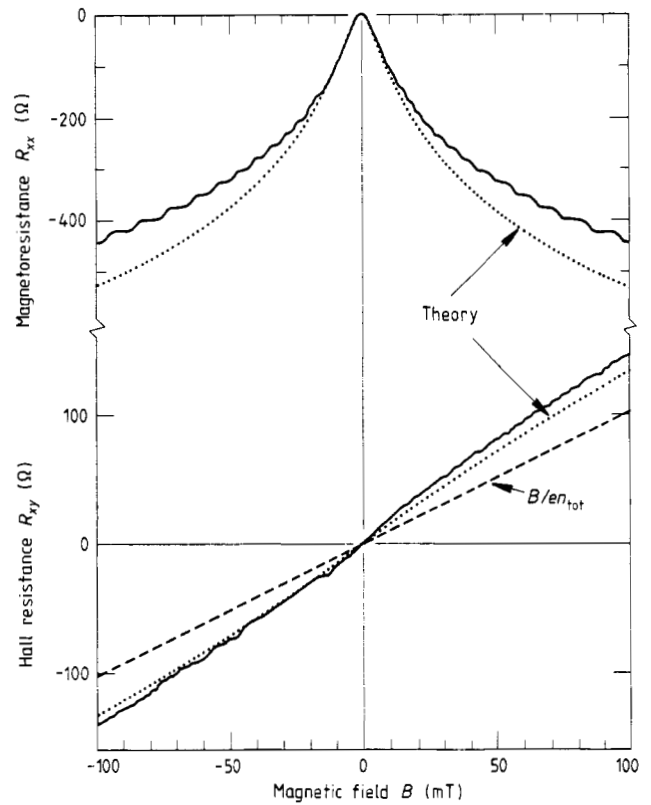


Figure 9. Low field weak localisation magnetoresistance $\Delta R_{xx}(B)$ and Hall resistance $R_{xy}(B)$ recorded for SDDH sample D as a function of magnetic field at $T = 0.35 \text{ K}$. The wiggles in the magnetoresistance are a result of analogue-to-digital conversion in our apparatus. A fit (dotted curve) to the theory of equations (1) and (2) (Hikami *et al* 1980) gives $B_\phi = 1.8 \text{ mT}$ and $\alpha = 2.0$. $B_0 = 95.8 \text{ mT}$ is determined from the square resistance and the charge carrier density. The broken line shows the free electron expectation based on the total charge-carrier density determined from the Shubnikov-de Haas effect.

correction is large means that the correction to the free electron Hall resistivity $R_{xy}(0) = B/(en_{\text{tot}})$ can be observed at low magnetic fields; this gives interesting additional information about the weak localisation, since it monitors the total quantum correction $\Delta\sigma(0, 0)$ in contrast to the negative magnetoresistance, which monitors $\Delta\sigma(0, 0) - \Delta\sigma(0, B)$, and the temperature dependence of the resistance displayed in figure 10, which monitors $\Delta\sigma(0, 0) - \Delta\sigma(T, 0)$. The correction to the Hall resistivity has not been reported previously in the literature.

A fit on the basis of equations (1) and (2) to the experimental curves is shown in figure 9 by the dotted curves. It should be noticed that equation (1) is valid only if $B \ll B_0$, in which region we find that the fit is indeed satisfactory. Only two adjustable parameters are involved, namely α and B_ϕ . The best fit gives $B_\phi = 1.8 \text{ mT}$ and $\alpha = 2$. The determination of α in this and in other cases precludes $\alpha = 1$ and strongly supports the picture of two independent 2D electron channels in our SDDH. For a similar sample (DQW450s) Harris *et al* (1988) came to the same conclusion based on a two-band analysis, which was relevant in their case due to the large difference in mobility of the two channels they observed.

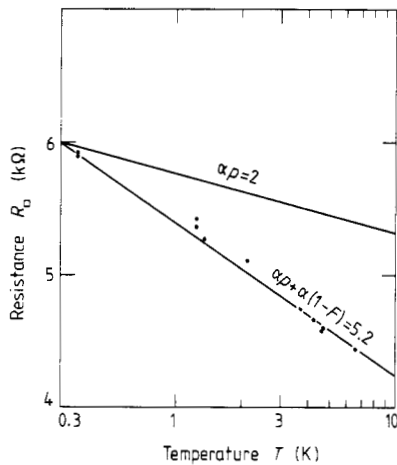


Figure 10. Resistance per square R_{xx} for SDDH sample F (also used for figures 6 and 7) plotted as a function of temperature in a semilogarithmic representation. Clearly $\Delta R_{xx} \sim \ln T$. Weak localisation predicts $\Delta R_{xx} \sim \alpha p \ln T$, where $\alpha = 2$ because of the two electron layers. p is the power dependence of the phase relaxation rate (or B_ϕ) as a function of temperature; we find $p = 1$. This expectation is shown ($\alpha p = 2$). With electron–electron interaction included we expect $\Delta R_{xx} \sim [\alpha p + \alpha(1 - F)] \ln T$, where $1 - F$ is the so-called interaction parameter. A fit to the experiment gives $1 - F = 1.6$. Other samples investigated also gave $1 - F > 1$.

As already mentioned there is one more way of detecting the weak localisation quantum correction, namely by measuring the temperature dependence of the resistivity at zero magnetic field. The resistivity is plotted as a function of the logarithm of temperature for sample F in figure 10. The linear variation is expected from equation (1). We can calculate the expected variation if we know α ($= 2$) and the power law T^p of the temperature dependence of B_ϕ . B_ϕ varies linearly with temperature, i.e. $p = 1$, and the expected variation of the resistance as a function of temperature is therefore the straight line in figure 10. There is, however, one more quantum correction to the resistivity, which is due to electron–electron interaction. This correction must account for the discrepancy. The temperature dependence of the resistivity with both correction included is of the form

$$R_{xx} = R_\square [1 + (\alpha R_\square e^2 / (\pi h)) p \ln T + (\alpha R_\square e^2 / (\pi h)) (1 - F) \ln T] \quad (3)$$

where the first term is due to weak localisation, and the second is due to electron–electron interaction in each layer. The factor α in front of each of the two logarithmic terms must be $\alpha = 2$ due to the existence of two 2D electron layers. The factor $(1 - F)$ to the last term is the so-called interaction parameter, and since everything else is fixed in equation (4), this is in fact what we determine. The surprising thing is that $(1 - F)$ is consistently larger than 1. In this case we find $(1 - F) = 1.6$. A similar discrepancy is found in the literature (Lin *et al* 1984) and is not understood at present. We expect that this quantum correction to the conductivity should also enhance

the Hall resistance as in equation (2b). It is difficult, however, to reconcile the experimental result in figure 9 with this large value of $1 - F$.

5. Conclusions

Two GaAs/AlGaAs heterostructures grown back to back gives an ideal system to study coupling between electronic 2D layers, since the layers grown by the modulation-doping technique can be formed in a intrinsic single-crystal GaAs/AlGaAs layer with far spacing to the nearest Si donor levels. We have made a study of the quantum Hall effect and the weak localisation effect in such a structure and found interesting new results, some of which are inherent to the double layer, and some will also be found in single 2D layers.

The most interesting result is the observation of fractional $i = \frac{1}{2}$ quantum Hall plateaus in the samples. The observation is supported by a series of experiments on etched double heterostructures where we clearly observe an imbalance between the two electronic sheets substantiating themselves in the Shubnikov–de Haas oscillations. A weak localisation correction to the resistivity is also consistent with the existence of two independent 2D electron layers, taken in the sense that electrons cannot cross from one layer to the other. Quantum corrections due to electron–electron interaction are observed but unfortunately they are not theoretically well understood.

Chakraborty and Pieliläinen (1987) have predicted the existence of an $i = \frac{1}{2}$ quantum Hall plateau for two 2D electron layers with a Coulomb coupling between the layers but no tunnelling. It is most likely this effect we observe, although the agreement is only semiquantitative. The energy gap at the $i = \frac{1}{2}$ filling of the lowest Landau level corresponds in classical terms to a correlated movement of the electrons in the two layers. The mutual effect of order through the interlayer electron–electron interaction generates the energy gap at $i = \frac{1}{2}$ occupation. The extra layer is like introducing order in the third dimension, which in turn stabilises electronic order in the planes. At even lower temperatures this may lead to the so-called electronic Wigner (1934) lattice. It would therefore be particularly interesting to study the behaviour of 2D electronic double layers at very low temperatures.

An additional novel observation concerns the low-field Hall resistivity, which we find to be non-linear as a function of magnetic field. This behaviour can be interpreted as the result of the inversion of the conductivity tensor with the weak localisation magnetoconductance included in the diagonal components of the tensor, yielding the observed effect in the off-diagonal components of the resistivity tensor. This effect samples the full weak localisation correction (as well as the electron–electron interaction term) and therefore gives an additional information to that obtained by the weak localisation magnetoresistance.

Acknowledgments

One of the authors (CBS) would like to thank Dr R Chow and Varian Ltd at Palo Alto for hospitality during the growth of several heterostructure wafers. Another author (RT) is grateful for a Carlsberg Scholarship for students. The research were supported by the Danish Science Research Council (SNF 11-4011), the Science for Technical Development Foundation (FTU 5.17.1.1.09) and the Danish Metrology Council (1986.725/000-25).

References

- Aoki H 1987 *Rep. Prog. Phys.* **50** 655
 Chakraborty T and Pietiläinen P 1987 *Phys. Rev. Lett* **59** 2784
 Eisenstein J P, Störmer H L, Narayanamurti V, Cho A Y, Gossard A C and Tu C W 1985 *Phys. Rev. Lett.* **55** 875
 Eisenstein J P, Willett R, Stormer H L, Tsui D C, Gossard A C and English J H 1988 *Phys. Rev. Lett.* **61** 997
 Fasol G, Mestres N, Hughes H P, Fischer A and Ploog K 1986 *Phys. Rev. Lett.* **56** 2517
 Harris J J, Lagemaat J M, Battersby S J, Hellon C M, Foxon C T and Lacklison D E 1988 *Semicond. Sci. Technol.* **3** 773
 Hawrylak P, Eliasson G and Quinn J J 1988 *Phys. Rev. B* **37** 10187
 Hikami S, Larkin A I and Nagaoka Y 1980 *Prog. Theor. Phys.* **63** 707
 Inoue K, Sakaki H and Yoshino J 1984 *Japan. J. Appl. Phys.* **23** L767
 Inoue K, Sakaki H, Yoshino J and Yoshioka Y 1985 *Appl. Phys. Lett.* **46** 973
 Lin B J F, Paalanen M A, Gossard A C and Tsui D C 1984 *Phys. Rev. B* **29** 927
 Miyatsuji K, Hihara H and Hamaguchi C 1985 *Superlatt. Microstruct.* **1** 43
 Nicholas R J, Brumme M A and Portal J C 1982 *Surf. Sci.* **113** 290
 Nørregaard J, Sørensen C B and Lindelof P E 1987 *Proc. 13th Nordic Semiconductor Meeting (Saltsjöbaden, Sweden) 1987* ed. M Östling (Stockholm: Royal Institute of Technology) p 285
 Pinczuk A, Lamont M G and Gossard A C 1986 *Phys. Rev. Lett.* **56** 2092
 Que W-M and Kirczenow G 1987 *J. Phys. C: Solid State Phys.* **20** L989
 Santoro G E and Giuliani G F 1988 *Phys. Rev. B* **37** 937
 Stormer H L, Eisenstein J P, Gossard A C, Wiegmann W and Baldwin K 1986 *Phys. Rev. Lett.* **56** 85
 Vinter B and Tardella A 1987 *Appl. Phys. Lett.* **50** 410
 Visscher P B and Falicov L M 1971 *Phys. Rev. B* **3** 2541
 Wigner E 1934 *Phys. Rev.* **46** 1002
 Yang R-Q, Lu X-J and Tsai C-H 1988 *J. Phys. C: Solid State Phys.* **21** L91